Role of Grain-to-Grain Contacts on Profiles of Retained Colloids in Porous Media in the Presence of an Energy Barrier to Deposition

XIQING LI,[†] CHEN-LUH LIN,[‡] JAN D. MILLER,[‡] AND WILLIAM P. JOHNSON*,[†]

Department of Geology & Geophysics, University of Utah, Salt Lake City, Utah 84112 and Department of Metallurgical Engineering, University of Utah, Salt Lake City, Utah 84112

Deposition of 36-μm gold-coated hollow microspheres in two porous media (glass beads and quartz sand, 710−850 μm) was examined using X-ray microtomography (XMT) in the presence of an energy barrier to deposition under fluid velocity conditions representative of engineered filtration systems. XMT allowed examination of the deposition at different locations at the grain surfaces (deposition at grain-to-grain contacts versus single-contact deposition). We demonstrate that in the presence of an energy barrier to deposition, grain-to-grain contacts strongly influence colloid deposition and the spatial distribution of retained colloids in porous media. This result contrasts drastically with observations in the absence of an energy barrier to deposition, where consistency with filtration theory was observed. In the presence of an energy barrier, colloids were dominantly retained at grain-to-grain contacts, and the concentration of retained particles varied nonmonotonically with transport distance. It is proposed that the nonmonotonic profiles resulted from translation of surface-associated microspheres and subsequent immobilization at grain-to-grain contacts. This hypothesis is demonstrated using a conceptual model. The mutability and sensitivity of retained profiles to system conditions (from hyper-exponential to nonmonotonic) may reflect the interplay of different deposition mechanisms under different conditions.

Introduction

Colloid transport in porous media is most commonly described by classic filtration theory (*1*−*4*), in which a spatially constant first-order deposition rate coefficient is estimated based on the physical attributes of the system. The assumed spatial invariance of the deposition rate coefficient yields exponential decreases in retained colloid concentrations with transport distance. In the absence of an energy barrier to deposition, e.g., for oppositely charged colloids and collectors (porous media grains), filtration theory predicts well the observed magnitude of the deposition rate coefficient and the observed exponential decrease in retained colloid concentrations (e.g., refs *5*−*7*). Filtration theory idealizes the porous media as a collection of spherical grains that are completely surrounded by fluid envelopes (*2*, *8*); whereas the packed structure in an actual porous media is supported via grain-to-grain contacts, and grains cannot, in reality, be completely surrounded by fluid. Despite this idealization, filtration theory clearly provides an excellent approximation of the deposition process in the absence of an energy barrier to deposition (e.g., refs *5*, *6*).

In the presence of a significant energy barrier to deposition (e.g., like-charged colloids and collectors), deposition is theoretically precluded by the repulsive colloid−collector interaction energy (e.g., ref *9*), whereas deposition is observed. A number of possible mechanisms exist by which to allow colloid deposition onto overall like-charged surfaces, e.g., surface roughness (*10*, *11*), surface charge heterogeneity (*9*, *12*−*15*), deposition in the weakly attractive energy minimum (secondary energy minimum) at greater separation distances than from the interaction energy barrier (*16*−*20*), and straining (physical entrapment in pore constrictions too small to pass) (*21*−*23*). Deposition "in" secondary energy minima requires the presence of physical features that allow colloids to be retained despite their loose association with grains surfaces which renders them subject to fluid drag. Retention of these secondary-minimum associated colloids has been thought to occur in so-called rear stagnation points on the downstream side of grains and asperities (*18*−*20*). However, it is also possible that grain-to-grain contacts serve as the zones in which secondary-minimum associated colloids are retained.

It has also been recently demonstrated that for deposition in the presence of an energy barrier, the concentrations of retained colloids do not decrease exponentially with distance from the source (e.g., refs *5*−*7*). The most commonly observed form of deviation from expectations from filtration theory is hyper-exponential (faster than exponential) decreases of retained colloid concentrations with transport distance (e.g., refs *5*, *7*, *24*, *25*). Recently, an increasing number of studies demonstrate nonmonotonic variation of retained colloid concentrations with transport distance (*6*, *26*−*30*). The form of deviation of the retained profile has been demonstrated to be highly sensitive to system conditions, and can switch from hyper-exponential to nonmonotonic as a result of minor changes in solution chemistry, or surface properties of the colloid or the porous media (*6*, *30*). The mechanisms that produce these deviations from filtration theory, and their mutability, are poorly understood. In the case of hyper-exponential deviations, heterogeneity in surface characteristics among the colloid population is a well-accepted mechanism to drive this deviation (*5*, *7*, *24*, *25*). At this time, no mechanism has been proposed to drive the observed nonmonotonic deviation.

Elucidation of the role of grain-to-grain contacts on colloid deposition requires direct observation at the pore-scale. To examine the resulting profile of retained colloids, pore-scale observation must be made across assemblage-scale domains, as provided by X-ray microtomography (XMT) (*31*). XMT investigations performed under conditions absent an energy barrier demonstrated that the presence of grain-to-grain contacts somewhat alters the environment of deposition, i.e., a significant fraction of deposition occurs in grain-to-grain contacts. However, the magnitude of the deposition rate coefficient and the spatial distribution of retained colloid concentrations were well predicted by filtration theory (*31*), demonstrating that the mechanism of colloid deposition was consistent with that assumed in filtration theory (collision with the grain surfaces). Therefore, in the absence of an energy barrier to deposition, filtration theory captures the essential

* Corresponding author phone: (801) 581-5033; fax: (801) 581-7065; e-mail: wjohnson@mines.utah.edu.

[†] Department of Geology & Geophysics, University of Utah.

[‡] Department of Metallurgical Engineering, University of Utah.

10.1021/es052501w CCC: $33.50
Published on Web 05/17/2006

elements of the deposition process despite a lack of accounting for grain-to-grain contacts.

The purpose of this paper is to demonstrate using XMT that in the presence of an energy barrier to deposition, near neutrally buoyant particles (36 μm) were dominantly retained at grain-to-grain contacts in two porous media (quartz sand and glass beads, 710−850 μm), and the profiles of retained particles deviated dramatically (nonmonotonically) from the exponential profiles expected from filtration theory. The observations demonstrate that the role of grain-to-grain contacts in deposition is drastically different in the presence versus the absence of an energy barrier to deposition. Relevance of these observations to smaller particles and colloids is discussed, and we demonstrate that the physicochemical mechanisms governing the deposition of these larger particles are equivalent to those governing the deposition of smaller particles and colloids. A conceptual model is presented to demonstrate a potential mechanism that yields the observed nonmonotonic profile of retained particles in the presence of an energy barrier.

Methods

Preparation of Gold-Coated Hollow Microspheres. Hollow ceramic microspheres (Trelleborg Fillite Inc., Norcross, GA) with an initial density range of 0.6−0.8 g-cm^{-3} were used as the starting material. The fraction of microspheres with sizes between 30 and 38 μm were separated using a stainless steel sieve (opening size 38 μm) and a mesh screen (opening size 30 μm). About 2 g of the separated fraction of microspheres were put into Milli-Q water (Millipore Corp. Bedford, MA) to remove whole from broken microspheres by flotation. The floating (whole) microspheres were dried in air, and put into ethyl ether (density 0.71 g-cm^{-3}) to further narrow the density range. Floating microspheres (density between 0.6 and 0.71 g-cm^{-3}) were filtered, rinsed with water, and air-dried.

About 0.05 g dried microspheres were spread evenly into an aluminum dish (diameter 2.5 in.) and placed into the vacuum chamber of the Denton Discovery-18 sputtering system (Denton Vacuum, Moorestown, NJ). Gold sputtering was performed at vacuum pressure less than 4×10^{-6} Torr. Following sputtering, the microspheres were suspended using ethanol, filtered, and rinsed sequentially with Milli-Q water and methanol. To produce negatively charged hydrophilic surfaces on the microspheres in aqueous solution, the methanol-rinsed gold-coated microspheres were reacted with 10 mL 5 mM mercaptoacetic acid (Sigma-Aldrich, St. Louis, MO) solution in methanol for at least 24 h. The treated gold-coated microspheres were filtered, rinsed repeatedly with water, and re-suspended into water in a 50 mL centrifuge tube. The fraction of microspheres with a density range between 1.06 and 1.26 g-cm^{-3} was separated (for column experiments) based on settling velocity calculation.

Porous Media. The porous media used in the column experiments was 20−25 mesh (average size 780 μm) soda lime glass beads (Cataphote Inc., Jackson, MS) and quartz sand (Fisher Scientific, Fair Lawn, NJ). The glass beads were first rinsed sequentially with acetone and hexane and then soaked with concentrated HCl for about 24 h, followed by repeated rinsing with Milli-Q water. The quartz sand was cleaned by soaking in concentrated HCl for at least 24 h, followed by repeated rinsing with ultrapure water, drying at 105 °C and baking overnight at 850 °C.

Column Experiment Conditions. Borosilicate glass columns (75 mm in length and 8 mm in inner diameter) were wet packed with the cleaned porous media to a packed length of 50 mm. Since the sample stage of the XMT facility cannot accommodate samples longer than 40 mm, the glass column consisted of two pieces (each 37 mm long) which can be scanned separately. The two pieces had flanges (2.5 mm thick) at one end to allow connection, which was sealed using Parafilm. The porosities of the packed glass beads and quartz sand was 0.404 and 0.376, respectively.

The packed columns were preequilibrated with about 20 pore volumes of degassed 5 μM polyoxyethylene (23) lauryl ether (Sigma-Aldrich, St. Louis, MO) solution at a pH of 10.5 (adjusted using NaOH). Polyoxyethylene lauryl ether was added to increase the height of the energy barrier to deposition (as evidenced by increased breakthrough concentrations relative to pure water at pH 10.5). One pore volume was equal to 1.01 and 0.94 mL for packed glass beads and quartz sand, respectively. Following preequilibration, two pore volumes of the gold-coated microsphere suspension were introduced in down-flow mode, followed by three pore volumes of elution with polyoxyethylene lauryl ether solution at pH of 10.5. The influent concentration of gold-coated microspheres was adjusted to 2.3×10^3 particles-mL^{-1}. During the experiments, the fluid level was maintained at a given distance above the top of the porous media and the column effluent outlet to ensure a constant pressure head and constant fluid velocity. The transport experiments were carried out at a pore water velocity of 0.1 cm-s^{-1}, and an additional experiment with quartz sand was run at a velocity of 0.25 cm-s^{-1}. These fluid velocities represent the flow conditions in engineered filtration systems (e.g., riverbank filtration and rapid sand filtration).

The concentrations of the effluent samples were determined by counting microspheres in 25 μL of effluent under a microscope after evaporation of water. For samples having low effluent concentrations, up to 200 μL effluent suspensions of the samples were counted.

Following the experiment, the two pieces of the column were separated, sealed at both ends using Parafilm, and scanned by XMT. The retained microspheres in the column were counted directly from the reconstructed XMT images. The mass balances were obtained by dividing the total number of microspheres recovered from effluent and retained in the column by the total number of microspheres introduced into the column. More details of gold-coated microsphere preparation and column experiments were provided in Li et al. (*31*).

XMT System and Scanning Procedures. After the column experiments, the two column pieces (with porous media containing microspheres) were scanned using the cone beam XMT system (Konoscope 40−130, Aracor Inc. Hawthorne, CA) at University of Utah. The device consists of a microfocus X-ray source, a sample positioning stage, and a digital X-ray detection camera. The power of the X-ray source tube was set at 16 W at which the focal spot was 20 μm in diameter. A computer-controlled vertical/rotary positioning system allowed the sample (column pieces) to rotate 0.72° and move 2.5 μm upward in vertical direction in the X-ray beam. The X-ray detection system consists of a fiberoptic taper, a scintillator/fiberoptic faceplate, and a CCD camera system. Details of the Konoscope XMT system can be found elsewhere (32).

Each scan produced projection data of packed porous media segments that are approximately 8 mm long. Since XMT cannot produce all projections for samples with a diameter greater than 10 mm, image reconstruction of the column at the flange connection (5 mm in length) was not possible. Six scans (segments) were required to obtain the projection data for the entire length of the column (45 mm), except the flange connection. The number of retained microspheres at the connection was interpolated by multiplying the average number retained in the 3 mm-long segments above and below the connection by a length correction factor of 1.67 (5 mm/3 mm). The projection data of each segment was used to reconstruct the image of the segment. Reconstruction was done with filtered back-

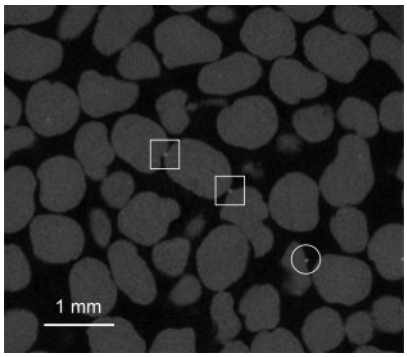

FIGURE 1. Representative cross-sectional XMT image of quartz sand (gray areas) and gold-coated hollow microspheres (white spots). Black areas represent pore water. The microsphere in the white circle demonstrates single contact retention. Microspheres in the white boxes are retained at grain-to-grain contacts.

projection algorithm, details of which are provided elsewhere (33).

Results and Discussion

Representative XMT Image. In the cross-sectional XMT image (Figure 1), gray areas represent porous media grains (quartz sand in this case), whereas black areas represent pore water. The white spots in boxes and the circle are microspheres retained grain-to-grain contacts and at non-contact areas, respectively. Retention at grain−wall contacts are considered equivalent to retention at grain-to-grain contacts. No microspheres were in contact simultaneously with three neighboring grains in either of the two porous media. Since straining is defined as physical entrapment of colloids by pore constrictions constrained by three neighboring porous media grains (*34*), our observation indicates that straining (as traditionally defined) did not occur in our system. That colloids retained at grain-to-grain contacts were held via two rather than three contact points indicates that the colloids were "wedged" between two surfaces in the presence of an energy barrier. This environment of deposition indicates that confinement of the colloid between the two collector surfaces allowed drag forces to overwhelm repulsive colloidal forces, thereby yielding direct contact with the bounding surfaces. Like straining, wedging is driven by physical confinement; however, we consider it useful to distinguish straining (deposition in pore constrictions too small to allow colloid passage) from wedging (confinement between two bounding surfaces).

Fraction of Retention at Grain-to-Grain Contacts. In both glass bead and quartz sand porous media, mass recoveries (>81%) were good under all conditions examined (Table 1). Absolute retention (total retained relative to total introduced) was much greater in the quartz sand relative to glass beads (fluid velocity = 0.1 cm-s^{-1}), as demonstrated by the percent retained of the total number introduced (61.5% in quartz sand, 2.0% in glass beads) (Table 1). Retention at grain-to-grain contacts was also much greater in the quartz sand (54.5%) relative to the glass beads (1.5%), where again the percents are relative to the total number introduced (Table 1).

In both porous media, retention occurred dominantly at grain−grain contacts. Of the total number retained, 75.0% and 88.6% were retained at grain-to-grain contacts in the glass beads and quartz sand, respectively (Table 1, Figure 2). In contrast, in the absence of an energy barrier, single-contact retention was dominant, with 20.1% and 41.4% of the total number retained being located at grain-to-grain contacts in the glass beads and quartz sand, respectively, at the same fluid velocity (*31*).

Retained Profiles. In both glass bead and quartz sand porous media, the total concentrations of retained microspheres varied nonmonotonically with transport distance (increased and then decreased). The peak concentration was located at a greater distance down-gradient from the column inlet in the glass beads (3.25 cm) relative to the quartz sand (1.25 cm). The down-gradient location of the peak concentration did not change with increased fluid velocity (from 0.1 to 0.25 cm-s^{-1}) in the quartz sand (Figure 3). This velocity increase yielded slightly increased absolute retention at grain−grain contacts, i.e., from 54.5 to 61.4% (of total injected) (Table 1). The nonmonotonic profiles obtained in the presence of an energy barrier to deposition provide dramatic contrast to the log-linear profiles obtained in the absence of an energy barrier (*31*).

Mechanism Causing the Nonmonotonic Retained Profiles. The sensitivity of the retained profile shape to solution conditions (in the absence vs presence of an energy barrier to deposition) demonstrates that these profile shapes are not artifacts of packing or hydrodynamic nonuniformity at the inlet of the column. Furthermore, the mutability of these profiles in response to solution conditions is consistent with previous work examining smaller biological and non-biological colloids in larger columns (e.g., *6*, *30*), demonstrating that the same physicochemical processes apply to both systems.

To the best of our knowledge, no mechanism has been proposed in the literature to explain the transition from hyperexponential to nonmonotonic retained profiles. Since the nonmonotonic retained profiles are produced in the presence of an energy barrier to deposition, it is reasonable to expect that colloid accumulation in the secondary energy minimum contributes to deposition under these conditions, as proposed by previous authors (*16*−*20*, *35*). The interaction energy profile between gold-coated microspheres and quartz sand surfaces was estimated using classic DLVO theory (*36*, *37*). The electric double-layer repulsive interaction and the retarded van der Waals attractive interaction were calculated based on the expressions developed by Gregory (*38*, *39*). The zeta potentials of the microspheres (−28.5 mV) and crushed quartz sand (−100 mV) were measured using micro-electrophoresis (Zetaplus Analyzer, Brookhaven Inc.). The decay length for the van der Waals interaction was 100 nm, and the Hamaker constant was 4.63×10^{-20} J. This Hamaker constant value was obtained by combining the Hamaker constants of gold (4.0×10^{-19} J) (*40*), water (3.7×10^{-20} J) (41), and quartz (8.86×10^{-20} J) (*42*). The secondary minimum depth was 4.8 kT, at a separation distance of 199 nm. A large energy barrier (2.96×10^{4} kT) existed at a separation distance of 12 nm, which was expected to preclude any single-contact deposition "within" primary energy minima in the absence of surface

TABLE 1. Column Experiment Conditions and Mass Recoveries[a]

porous media	fluid velocity (cm-s^{-1})	total deposition (%[b])	deposition at G−G (%)[b]	fraction at G−G (%)[c]	effluent recovery (%)[b]	mass recovery (%)
glass beads	0.1	2.0	1.5	75.0	91.3	93.3
quartz sand	0.1	61.5	54.5	88.6	19.8	81.3
quartz sand	0.25	72.6	61.4	84.6	15.8	88.4

[a] "G-G" represents grain-to-grain contacts. [b] relative to total number of microspheres introduced. [c] relative to total number deposited.

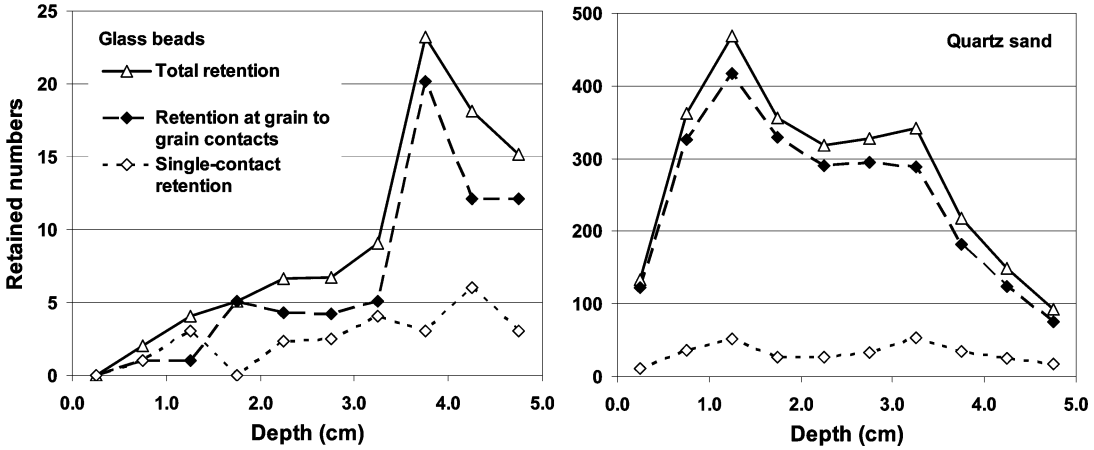

FIGURE 2. Profiles of total retention, grain-to-grain contact retention, and single-contact retention in glass beads and quartz sand (pore water velocity = 0.1 cm-s^{-1}). Note that the scales for *y*-axis are different for the two porous media.

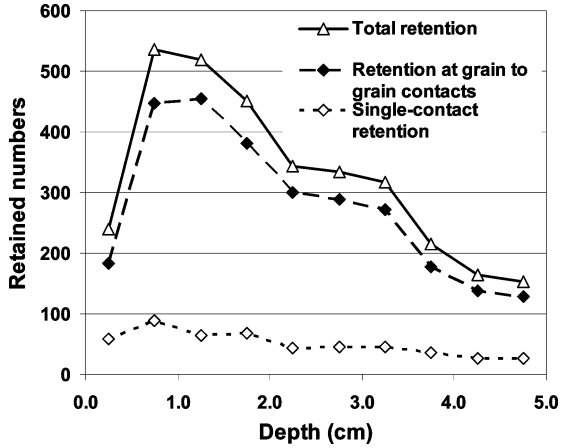

FIGURE 3. Profiles of total retention, grain-to-grain contact retention, and single-contact retention in quartz sand at a fluid velocity of 0.25 cm-s^{-1}.

nonidealities (e.g., surface charge heterogeneity and surface roughness) that might locally reduce or eliminate the energy barrier to deposition.

The concurrence of dominant deposition at grain-to-grain contacts and nonmonotonic profiles of retained colloids indicates an association between the two phenomena. Although this association is not necessarily causal, the potential cause and effect relationship is worth considering. The "loose" association of colloids with grain surfaces via the secondary energy minimum makes them subject to fluid drag and down-gradient translation (*18*−*20*). Down-gradient translation of secondary minimum-associated colloids was recently demonstrated in an impinging jet system (15). In porous media, down-gradient translation of secondary-minimum associated colloids may lead them to grain-to-grain contacts where they may become immobilized due to wedging. The possibility that surface-associated particles migrate to, and are retained at, grain-to-grain contacts is supported by the observation that absolute deposition at grain−grain contacts in quartz sand (fluid velocity = 0.1 cm-s^{-1} was greater in the presence (54.5%) relative to the absence (41.4%) of an energy barrier to deposition (the latter value comes from ref *31*). This difference indicates that a portion of microspheres that would have been immobilized via single-contact deposition in the absence of an energy barrier were instead captured (e.g., via wedging) at grain-to-grain contacts in the presence of an energy barrier. That is, these microspheres have migrated to grain-to-grain contacts. Down-gradient migration of microspheres in the presence of an energy barrier to deposition is also supported by the observation that retention at grain-to-grain contacts over the first 1.5 and 3.0 cm transport distance in quartz sand and glass beads, respectively (fluid velocity = 0.1 cm-s^{-1}), was greater in the absence relative to the presence of an energy barrier, whereas retention at grain-to-grain contacts at greater transport distances was greater in the presence relative to the absence of an energy barrier (ref *31* and Figure 2).

Based on the above observations, we propose that the nonmonotonic profiles reflect the interplay of two processes: (1) down-gradient migration of secondary energy minimum-associated colloids and increased likelihood of retention at grain-to-grain contacts with increased migration; (2) depletion of secondary minimum-associated colloids with increased down-gradient distance due to retention up-gradient. This concept is demonstrated using a simple conceptual model that tracks the migration and retention of surface-associated colloids, and considers the aqueous phase solely as a steady-state source of colloids to the surface-associated phase.

Increased likelihood of retention at grain-to-grain contacts with increased migration was included, implicitly, in the conceptual model by immobilizing a fraction of the secondary minimum-associated colloids in each segment. The likelihood of immobilization was constant within a given segment, yielding an overall increased probability of immobilization for each subsequent segment entered. Depletion of secondary-minimum associated colloids with increased transport distance resulted directly from immobilization, as well as by depletion of colloids in the bulk mobile phase due to association with surfaces via the secondary energy minimum.

The number of colloids entering the surface-associated phase from the aqueous phase in each segment (S_n) during each time step was decreased hyper-exponentially with distance down-gradient of the first segment (S_1), to reflect retained profiles often observed in the presence of an energy barrier, as described above. A fraction (f_d) of the surface-associated colloids was immobilized in each segment at each time step, yielding a number of retained colloids, which represented colloids immobilized at grain-to-grain contacts. Mobile surface-associated colloids migrated to adjacent down-gradient segments where they were subject to the same likelihood of immobilization (f_d). The surface-associated phase in all segments down-gradient of the first segment gained colloids from both the aqueous phase and the surface-associated phase in the up-gradient segment. Colloid re-entrainment was not considered, to be consistent with experiments demonstrating that the nonmonotonic retained profiles develop in the absence of significant re-entrainment (e.g., ref *6*).

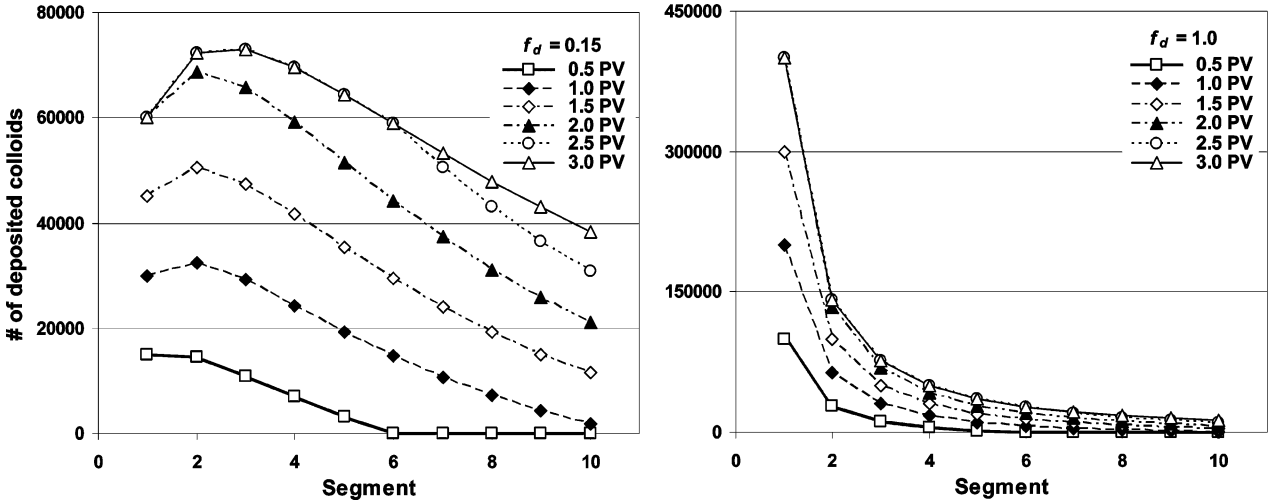

FIGURE 4. Evolution of the profiles of retained colloid concentrations over distance. Deposited colloid concentrations were developed using a simple conceptual model that considers migration of surface-associated colloids and subsequent immobilization (e.g., at grain-to-grain contacts). "PV" represents pore volume.

Since the model is purely conceptual, physically based travel distances and velocities are not utilized. Rather, arbitrary values are utilized to demonstrate the concept. For purposes of illustration, a value of 20 000 was used for S_1, and a value of −1.5 was used as the exponential coefficient in the expression of S_n:

$$S_n = S_1 n^{-1.5}$$

where n represents nth segment. The value of f_d was constant for all model segments, and was set equal to either 0.15 or 1.0 to demonstrate the effect on the resulting profile of retained colloids. Simulations involved "injection" for two pore volumes followed by "elution" for one pore volume, where each pore volume was composed of 10 time steps (since the column is comprised of 10 segments). The simulation was performed using a spreadsheet.

The parameters used here yielded either a nonmonotonic or hyper-exponential profile before the first pore volume was introduced, as shown in Figure 4, where the retained profile is shown for various times during the simulation for the case where $f_d = 0.15$ (left) and $f_d = 1.0$ (right). f_d equal to unity indicates all surface-associated colloids are instantaneously immobilized. During additional pore volumes of "injection", steady-state deposition was achieved and the profile shapes remained constant as their magnitudes increased (Figure 4). During the first pore volume of elution, bulk phase and surface-associated colloids continued to migrate along the column. Some of them were immobilized, thereby increasing the retained concentrations on down-gradient segments (Figure 4 left). Following one pore volume of elution, all retained colloids were immobile, and the peak-retained colloid concentration did not shift down-gradient with further elution, consistent with experimental observations where re-entrainment was negligible (*6*). The resulting retained profiles demonstrated two characteristic shapes: nonmonotonic ($f_d = 0.15$), and hyper-exponential ($f_d = 1.0$), indicating that mobility of surface-associated colloids and subsequent immobilization at grain-to-grain contacts is one possible explanation for the observed transition from hyper-exponential to nonmonotonic retained profiles.

The location of the peak concentration depends on the value of f_d, where lower values yield less deposition and peaks that are located farther down-gradient from the column inlet (Figure 5), a result that agrees with the observation that, in glass beads, the magnitude of deposition was lower, and the location of the peak was farther down-gradient, relative to

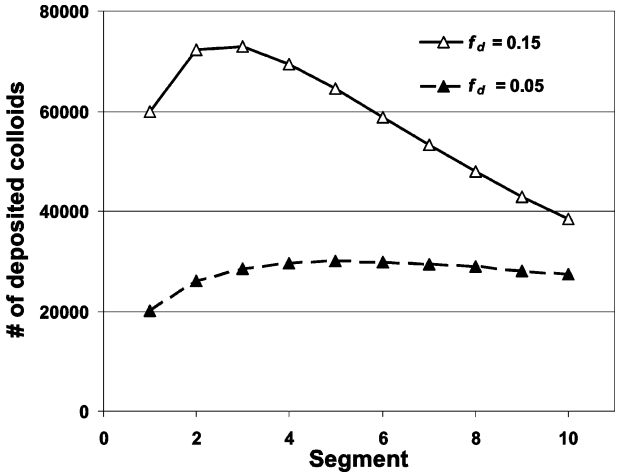

FIGURE 5. Profiles of retained colloid concentration at end of the elution for different values of f_d. Lower f_d (lower likelihood of capture of surface-associated colloids in a segment) is more likely in glass beads than in quartz sand, due to the lower numbers of grain-to-grain contacts per grain, and the shorter average length of grain-to-grain contacts.

the quartz sand. The likelihood of immobilization in grain-to-grain contacts is expected to be lower in the glass beads relative to the quartz sand due to the lower number of grain-to-grain contacts per grain, and the shorter average length of grain-to-grain contacts in that porous media relative to the quartz sand (*31*).

Relevance of grain-to-grain contacts to smaller colloids is demonstrated by equivalent responses to the absence versus the presence of an energy barrier for both the large and the small colloids. In the absence of an energy barrier the magnitude of deposition was well-predicted by filtration theory for both colloid sizes (*5*−*7*, *31*), and the concentration of retained colloids decreased log-linearly with transport distance. In the presence of an energy barrier to deposition, the concentration of retained colloids decreased nonmonotonically with transport distance (*6*, *30*). These similarities indicate that equivalent physicochemical processes governed the deposition of colloids in both systems.

The mutability of retained profiles, that is, the sensitivity of retained profile shape (e.g., hyper-exponential versus nonmonotonic) to system conditions (*6*, *30*) suggests that colloid deposition occurs via multiple mechanisms in a given porous medium, and that the dominance of particular

mechanisms yields particular profile shapes. The hyperexponential retained profiles may be associated with lack of colloid mobility once the colloid is associated with the surface, e.g., via deposition at locations where an energy barrier is locally absent (e.g., deposition "in" primary energy minima via surface charge heterogeneities). Colloids associated with the surface via secondary energy minima are mobile (*15*, *18*−*20*). These mobile colloids may eventually become immobilized at grain-to-grain contacts, rear stagnation zones, and locations where the energy barrier is locally absent, yielding a nonmonotonic retained profile. Under the conditions examined here, grain-to-grain contacts were most important. Since these various mechanisms of deposition are sensitive to solution conditions, surface properties of the colloids, and surface properties of the collectors, it is not surprising that the profile shapes are sensitive to system conditions.

Acknowledgments

This material is based upon work supported by the National Science Foundation Hydrologic Sciences Program (EAR 0337258). Any opinions, findings, and conclusions or recommendations expressed in this material are those of the author(s) and do not necessarily reflect the views of the National Science Foundation. X.L. wishes to thank Minjian Yu at the Department of Family and Consumer Studies of the University of Utah for her help with the column experiments.

Literature Cited

(1) Yao, K. M.; Habibian, M. T.; O'Melia, C. R. Water and wastewater filtration: Concepts and applications. *Environ. Sci. Technol.* **1971**, *5*(11), 1105−1112.
(2) Rajagopalan, R.; Tien, C. Trajectory analysis of deep-bed filtration with the sphere-in-cell porous media model. *AIChE J.* **1976**, *22*(3), 523−533.
(3) Tufenkji, N.; Elimelech, M. Correlation equation for predicting single-collector efficiency in physicochemical filtration in saturated porous media. *Environ. Sci. Technol.* **2004**, *38*, 529−536.
(4) Nelson, K. E.; Ginn, T. R. Colloid filtration theory and the Happel sphere-in-cell model revisited with direct numerical simulation of colloids. *Langmuir* **2005**, *21*(6), 2173-2184.
(5) Li, X.; Scheibe, T. D.; Johnson, W. P. Apparent decreases in colloid deposition rate coefficient with distance of transport under unfavorable deposition conditions: a general phenomenon. *Environ. Sci. Technol.* **2004**, *38*(21), 5616−5625.
(6) Li, X.; Johnson, W. P. Nonmonotonic variations in deposition rate coefficients of microspheres in porous media under unfavorable deposition conditions. *Environ. Sci. Technol.* **2005**, *39*(6), 1658−1665.
(7) Tufenkji, N.; Elimelech M. Deviation from classical colloid filtration theory in the presence of repulsive DLVO interactions. *Langmuir* **2004**, *20*, 10818−10828.
(8) Happel, J. Viscous flow in multiparticle systems: slow motion of fluids relative to beds of spherical particles. *AIChE J.* **1958**, *4*(2), 197−201.
(9) Elimelech, M.; O'Melia, C. R. Kinetics of deposition of colloidal particles in porous media. *Environ. Sci. Technol.* **1990**, *24*(10), 1528−1536.
(10) Bhattacharjee, S.; Ko, C. H.; Elimelech, M. DLVO interaction between rough surfaces. *Langmuir* **1998**, *14*, 3365−3375.
(11) Shellenberger, K.; Logan, B. E. Effect of molecular scale roughness of glass beads on colloidal and bacterial deposition. *Environ. Sci. Technol.* **2002**, *36*(2), 184−189.
(12) Song, L.; Elimelech, M. Dynamics of colloid deposition in porous media: modeling the role of retained particles. *Colloid Surf., A* **1993**, *73*, 49−63.
(13) Song, L.; Elimelech, M. Transient deposition of colloidal particles in heterogeneous porous media. *J. Colloid Interface Sci.* **1994**, *167*, 301−313.
(14) Johnson, P. R.; Sun, N.; Elimelech, M. Colloid transport in geochemically heterogeneous porous media: Modeling and measurements. *Environ. Sci. Technol.* **1996**, *30*(11), 3284−3293.
(15) Johnson, W. P.; Tong, M. Simulated and experimental influence of hetero-domain size on colloid deposition efficiencies on overall like-charged surfaces. *Environ. Sci. Technol.* **2006**, in review.
(16) Hahn, M. W.; Abadzic, D.; O'Melia, C. R. Aquasols: On the role of secondary minima. *Environ. Sci. Technol.* **2004**, *38*, 5915−5924.
(17) Hahn, M. W.; O'Melia, C. R. Deposition and reentrainment of Brownian particles in porous media under unfavorable chemical conditions: some concepts and applications. *Environ. Sci. Technol.* **2004**, *38*, 210−220.
(18) Redman, J. A.; Walker, S. L.; Elimelech, M. Bacterial adhesion and transport in porous media: role of the secondary energy minimum. *Environ. Sci. Technol.* **2004**, *38*, 1777−1785.
(19) Walker, S. L.; Redman, J. A.; Elimelech M. Role of Cell Surface Lipopolysaccharides (LPS) in *Escherichia coli* K12 Adhesion and Transport. *Langmuir* **2004**, *20*, 7736−7746.
(20) Brow, C.; Li, X.; Ricka, J.; Johnson, W. P. Comparison of microsphere deposition in porous media versus simple shear systems. *Colloids Surf., A* **2005**, *253*, 125−136.
(21) Bradford, S. A.; Yates, S. R.; Bettahar, M.; Simunek, J. Physical factors affecting the transport and fate of colloids in saturated porous media. *Water Resour. Res.* **2002**, *38*(12), 1327−1338.
(22) Bradford, S. A.; Bettahar, M.; Simunek, J.; van Genuchten, M. Th. Straining and attachment of colloids in physically heterogeneous porous media. *Vadose Zone J.* **2004**, *3*, 384−394.
(23) Tufenkji, N.; Ryan, J. N.; Harvey, R. W.; Elimelech M. Transport of Cryptosporidium Oocysts in Porous Media: Role of Straining and Physico-Chemical Filtration. *Environ. Sci. Technol.* **2004**, *38*, 5932−5938.
(24) Albinger, O.; Biesemeyer, B. K.; Arnold, R. G.; Logan, B. E. Effect of bacterial heterogeneity on adhesion to uniform collectors by monoclonal populations. *FEMS Microbiol. Lett.* **1994**, *124*, 321−326.
(25) Simoni, S. F.; Harms, H.; Bosma, T. N. P.; Zehnder, A. J. B. Population heterogeneity affects transport of bacteria through sand columns at low flow rates. *Environ. Sci. Technol.* **1998**, *32*, 2(14), 2100−2105.
(26) Bolster, C. H.; Mills, A. L.; Hornberger, G.; Herman, J. Spatial distribution of deposited bacteria following miscible displacement experiments in intact cores. *Water Resour. Res.* **1999**, *35*, 1797−1807.
(27) Redman, J. A.; Grant, S. B.; Olson, T. M.; Estes, M. K. Pathogen filtration, heterogeneity, and the potable reuse of wastewater. *Environ. Sci. Technol.* **2001**, *35*(9), 1798−1805.
(28) Redman, J. A.; Estes, M. K.; Grant, S. B.; Resolving macroscale and microscale heterogeneity in pathogen filtration. *Colloids Surf., A* **2001**, *191*, 57−70.
(29) Harter, T.; Wagner, S.; Atwill, E. R.; Colloid transport and filtration of cryptosporidium parvum in sandy soils and aquifer sediments. *Environ. Sci. Technol.* **2000**, *34*(1), 62−70.
(30) Tong, M.; Li, X.; Brow, C.; Johnson. W. P. Detachment-influenced transport of an adhesion-deficient bacterial strain within water-reactive porous media. *Environ. Sci. Technol.* **2005**, *39*(8), 2500−2508.
(31) Li, X.; Lin, C. L.; Miller, J.; Johnson, W. P. Pore-scale observation of microsphere deposition at grain-to-grain contacts over assemblage-scale porous media using X-ray microtomography. *Environ. Sci. Technol.* **2006**, *40*, ****.
(32) Lin, C. L.; Miller, J. D. Cone beam X-ray microtomography—A new facility for 3D analysis of multiphase materials. *Miner. Metall. Process.* **2002**, *19*(2), 65−71.
(33) Feldcamp, L. A.; Davis, L. C.; Kress, J. W. Practical cone-beam algorithm. *J. Opt. Soc. Am.* **1984**, *1*(6), 612−619.
(34) Herzig, J. P.; Leclerc, D. M.; LeGoff, P. Flow of suspensions through porous media: application to deep filtration. *Ind. Eng. Chem.* **1970**, *62*, 8−35.
(35) Derjaguin, B. V.; Landau, L. Theory of the stability of strongly charged lyophobic sols and of the adhesion of strongly charged particles in solutions of electrolytes. *Acta Physicochim URSS* **1941**, *14*, 633−662.
(36) Verwey, E. J. W.; Overbeek, J. T. G. *Theory of the stability of lyophobic colloids;* Elsevier: Amsterdam, 1948.
(37) Gregory, J. Interaction of unequal double layers at constant charge. *J. Colloid Interface Sci.* **1975**, *51*, 44−51.
(38) Gregory, J. Approximate expressions for retarded van der Waals interaction. *J. Colloid. Interface. Sci.* **1981**, *83*, 138−145.
(39) Adamson, A. W. *Physical Chemistry of Surfaces,* 5th ed.; Wiley: New York and London, 1990.
(40) Bergendahl, J.; Grasso, D.; Prediction of colloidal detachment in a model porous media: thermodynamics. *AIChE J* **1999**, *45*(3), 475−484.
(41) Bergstrom, L.; Hamaker constants of inorganic materials. *Adv. Colloid Interface Sci.* **1997**, *70*, 125−169.

Received for review December 13, 2005. Revised manuscript received April 10, 2006. Accepted April 13, 2006.

ES052501W